LETTERS

Sub-cycle switch-on of ultrastrong light–matter interaction

G. Günter[1], A. A. Anappara[1,2], J. Hees[1], A. Sell[1], G. Biasiol[3], L. Sorba[2,3], S. De Liberato[4,5], C. Ciuti[4], A. Tredicucci[2], A. Leitenstorfer[1] & R. Huber[1]

Controlling the way light interacts with material excitations is at the heart of cavity quantum electrodynamics (QED). In the strong-coupling regime, quantum emitters in a microresonator absorb and spontaneously re-emit a photon many times before dissipation becomes effective, giving rise to mixed light–matter eigenmodes[1–12]. Recent experiments[13] in semiconductor microcavities reached a new limit of ultrastrong coupling[14], where photon exchange occurs on timescales comparable to the oscillation period of light. In this limit, ultrafast modulation of the coupling strength has been suggested to lead to unconventional QED phenomena[14,15]. Although sophisticated light–matter coupling has been achieved in all three spatial dimensions, control in the fourth dimension, time, is little developed. Here we use a quantum-well waveguide structure to optically tune light–matter interaction from weak to ultrastrong and turn on maximum coupling within less than one cycle of light. In this regime, a class of extremely non-adiabatic phenomena becomes observable. In particular, we directly monitor how a coherent photon population converts to cavity polaritons during abrupt switching. This system forms a promising laboratory in which to study novel sub-cycle QED effects and represents an efficient room-temperature switching device operating at unprecedented speed.

Microcavities enclosing a material resonance provide an elegant way to tailor the strength of light–matter interaction, quantified by the vacuum Rabi frequency, Ω_R. Intuitively, Ω_R represents the rate at which a photon is exchanged between an optical transition and a cavity mode through spontaneous emission and absorption. The following three regimes are distinguished. (1) For weak coupling, the discrete density of photonic states modifies the radiative lifetime of the material excitation (Purcell effect[16]). (2) If Ω_R exceeds the dissipation rates of light and matter fields, two polariton branches emerge as new eigenstates featuring an energy splitting of $2\hbar\Omega_R$, where $\hbar$ denotes Planck's constant divided by 2π. This strong-coupling regime has been investigated in diverse systems, ranging from atoms[1,2] through excitons in semiconductor quantum wells[3] and quantum dots[5,9] to Cooper-pair boxes[6,10]. Exciting perspectives arise for quantum information processing[5,6,10], lasing without inversion[17] and polaritonic Bose–Einstein condensation[17,18]. (3) Most recently, the giant dipole moments of intersubband transitions in quantum wells[19] have allowed for ultrastrong light–matter coupling[13–15]. Here Ω_R is large enough to amount to a significant fraction of the transition frequency, ω_{12} (for example, $2\Omega_R/\omega_{12} = 0.2$ in ref. 13).

In this regime, anti-resonant terms of the interaction Hamiltonian, usually accounted for in strongly driven systems only, become relevant even in equilibrium. The ground state is predicted to be a squeezed vacuum containing a finite number of virtual photons[14]. As long as the

quanta are confined inside the cavity, their unconventional nature remains hidden. Theory shows that non-adiabatic switching of Ω_R, introducing changes on a timescale shorter than the cycle of light, may release these virtual quanta in correlated pairs[14,15]. This example reveals a fundamental weakness of state-of-the-art light–matter control: up to now, non-adiabatic phenomena have remained an academic curiosity because there has been no laboratory capable of controlling light–matter interaction on a sub-cycle scale. Electronic tuning by means of an external gate voltage is clearly too slow[7]; theoretical proposals to modulate the dielectric constant of a cavity or the reflectivity of a mirror[20] have not been implemented for the required timescale either.

We introduce an all-optical scheme for femtosecond control of ultrastrongly coupled cavity polaritons—a test bed for targeting non-adiabatic light–matter interaction. The idea is sketched in Fig. 1. For maximum modulation depth, we start with an empty microcavity (Fig. 1a) and turn on coupling by direct injection of the emitter itself (Fig. 1b). Our sample contains 50 identical, undoped GaAs quantum wells separated by $Al_{0.33}Ga_{0.67}As$ barriers (Fig. 1c). The electronic wavefunctions are quantized along the growth direction forming subbands $|1\rangle$ and $|2\rangle$, which are unpopulated in thermal equilibrium. Radiative transitions between the subbands become possible only if electrons are injected into the first subband. The intersubband absorption line is centred at $\hbar\omega_{12} = 113\,\text{meV}$ (wavelength, $\lambda = 11\,\mu m$) with a dipole moment oriented along the growth direction. We embed the quantum wells in a planar waveguide for mid-infrared radiation. The effective thickness of the structure corresponds to $\lambda/2$ at an internal propagation angle of $\theta = 65°$. Hence, photon modes with electric field components in the growth direction (TM polarization) couple resonantly to intersubband transitions as long as the subbands are populated. The vacuum Rabi frequency is known to scale with the electron sheet density, N_e, in level $|1\rangle$ as $\Omega_R \propto \sqrt{N_e}$ (refs 7, 14, 15). In previous work, N_e was provided by static doping or electronic injection, both of which are difficult to modulate with high bandwidths. We employ a 12-fs control pulse centred at a photon energy of 1.55 eV to excite electrons resonantly from the valence band into conduction subband $|1\rangle$ (Fig. 1c). Because the inverse frequency of the intersubband transition is 37 fs, we activate it within less than half a cycle of light.

The eigenmodes of this system are resonantly sampled by reflectance of a phase-stable mid-infrared pulse (blue curve, Fig. 1c) coupled through the prism-shaped substrate. To achieve sub-cycle resolution, the real-time oscillations of the probe field are mapped out by phase-matched electro-optic detection[21]. Such ultrabroadband terahertz optoelectronics (refs 22, 23 and references therein) has proved to be a powerful tool for investigating the field response of
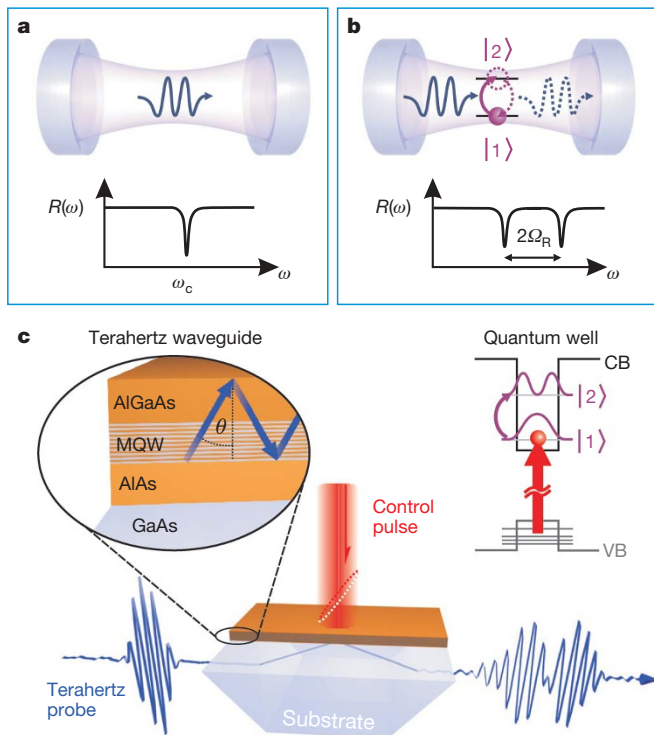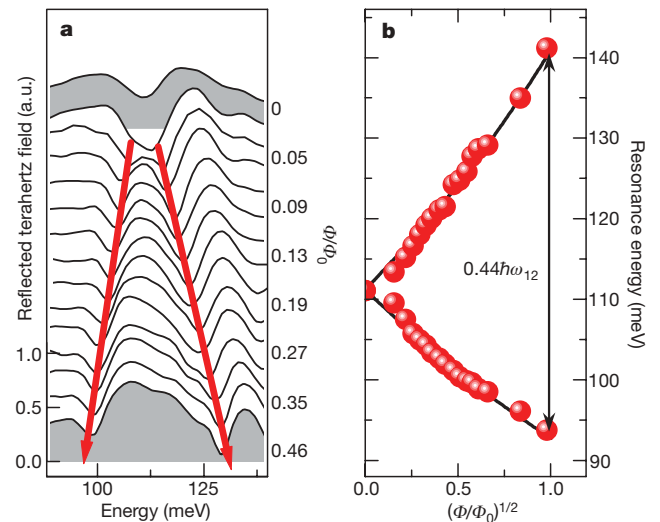
Figure 1 | Femtosecond control of ultrastrong light–matter coupling. a, A bare microcavity has minimal reflectance, $R(\omega)$, at the photon resonance, ω_c. **b,** After introduction of a resonant material excitation, cavity photons (blue) are coherently absorbed and re-emitted at rate Ω_R, giving rise to anticrossing cavity polaritons. **c,** A multiple quantum well structure (MQW) comprising 50 undoped GaAs wells (thickness, 9 nm) separated by $Al_{0.33}Ga_{0.67}As$ barriers (thickness, 30 nm) are embedded into a planar waveguide structure based on total internal reflection at the $Al_{0.33}Ga_{0.67}As$–air and AlAs–GaAs interfaces, respectively (magnified view). The quantum wells are positioned at the field antinode. The sketched band diagram (CB, conduction band; VB, valence band) shows how electronic transitions between subbands $|1\rangle$ and $|2\rangle$ (level spacing, $\hbar\omega_{12} = 113$ meV) are activated by near-infrared, 12-fs control pulses (photon energy, 1.55 eV; vertical red beam) populating level $|1\rangle$. Intersubband transitions may then resonantly couple to TM-polarized mid-infrared cavity photons propagating at $\theta = 65°$. Few-cycle TM-polarized multi-terahertz transients guided through the prism-shaped substrate are reflected from the waveguide to probe the ultrafast build-up of light–matter coupling in the system. The pulse front of the near-infrared control is tilted (dotted white circle in control beam) to match the geometry of the phase planes of the probe.

Figure 2 | Ultrawide optical tuning of light–matter interaction. a, Terahertz reflectance spectra measured at room temperature (293 K) for various fluences, Φ (vertically off-set), of the control pulse ($t_D = 20$ ps). Minima indicate eigenmodes of the system. For $\Phi = 0$, only the bare photon mode is observed, at $\hbar\omega_c = 113$ meV; both branches of the intersubband cavity polaritons are discernible for $\Phi \gtrsim 0.05\Phi_0$ ($\Phi_0 = 0.1$ mJ cm^{-2}). a.u., arbitrary units. **b,** Asymmetric polariton splitting as a function of Φ: dots, experiment; solid lines, simulation including anti-resonant light–matter interaction. For $\Phi = \Phi_0$, the polariton branches are observed with a relative energy distance of $0.44\hbar\omega_{12}$ for a given angle, $\theta = 65°$. This value corresponds to $2\Omega_R = 0.18\omega_{12}$. We estimate the maximum electron density to be on the order of 2×10^{12} cm^{-2}, consistent with the static doping concentrations of ref. 13. The spectra are obtained by Fourier transformation of time-domain data shown in Supplementary Fig. 1.

extremely non-equilibrium semiconductor systems[24–26]. Eigenmodes of the cavity cause characteristic minima in the Fourier spectra of the reflected transients. All experiments are performed under ambient conditions.

Figure 2a shows that the magnitude of the light–matter coupling is continuously tunable by means of the control fluence, Φ. The spectra are recorded at a fixed delay, $t_D = 20$ ps, between the near-infrared control and the multi-terahertz probe pulse. In equilibrium ($\Phi = 0$), a single reflectance minimum at $\hbar\omega_c = 113$ meV (top curve, Fig. 2a) attests to the sole resonance of the unexcited cavity, the bare photon mode. With increasing fluence, the system traverses all three regimes of light–matter interaction. Starting with weak coupling ($\Phi \lesssim 0.03\Phi_0$), Ω_R already exceeds the widths (full-width at half-maximum, ~5 meV) of intersubband and cavity resonances for $\Phi > 0.05\Phi_0$, and two strongly coupled cavity polariton branches are discernible. Further increase of the fluence enhances the separation of the minima to 50 meV, corresponding to a fraction of 44% of the bare photon frequency (Fig. 2b). As discussed in ref. 13, the apparent mode separation is not identical to the vacuum Rabi splitting at the anticrossing point. Only a quantitative simulation of the

energy position of the polariton dips (Fig. 2b) allows for extraction of Ω_R. For a correct description of our data, the theory has to go beyond the rotating-wave approximation[14,15]. We include anti-resonant terms in the light–matter Hamiltonian that scale with the ratio $2\Omega_R/\omega_{12}$. These contributions describe the simultaneous creation or annihilation of two excitations with opposite in-plane wavevectors **k** and give rise to a two-mode squeezed quantum vacuum[14,15]. By comparison with this theory, we determine that $2\Omega_R = 0.18\omega_{12}$ for our experiment. This value is comparable to the record achieved in delta-doped structures[13] and large enough for the signatures of ultra-strong coupling to be observable[14]. The scheme is expected to be scalable further by means of higher control fluences and a larger number of quantum wells.

The central issue is to explore how rapidly ultrastrong coupling may be activated. Figure 3 displays amplitude spectra recorded at various delay times, t_D ($\Phi = \Phi_0$). For $t_D \lesssim -50$ fs, the cavity resonance (blue arrow, Fig. 3) shows a minimum amplitude reflectivity below 10%. The control pulse induces dramatic reflectivity changes of order one, on the femtosecond scale. The initial bare photon state is replaced by two coupled polariton branches appearing simultaneously at energy positions of 93 meV and 143 meV (red arrows, Fig. 3). Most notably, the new resonances do not develop by gradual bifurcation of the bare cavity mode as in Fig. 2a. By contrast, switching occurs discontinuously once the control pulse promotes electrons into subband $|1\rangle$.

Immediately following the femtosecond control, the photoexcited charge carriers are in a highly non-equilibrium state which may induce enhanced dephasing of the intersubband transition. A detailed microscopic description of the switching dynamics should thus account for both the quantum kinetic aspects as well as the dynamics of the ultrastrong cavity–intersubband coupling. Notably, for the large coupling strengths achieved in our experiment, we find that dephasing arising from the non-equilibrium nature of the carrier distributions appears to be less important than the dynamics of the cavity polariton splitting. The instantaneous activation of light–matter interaction is
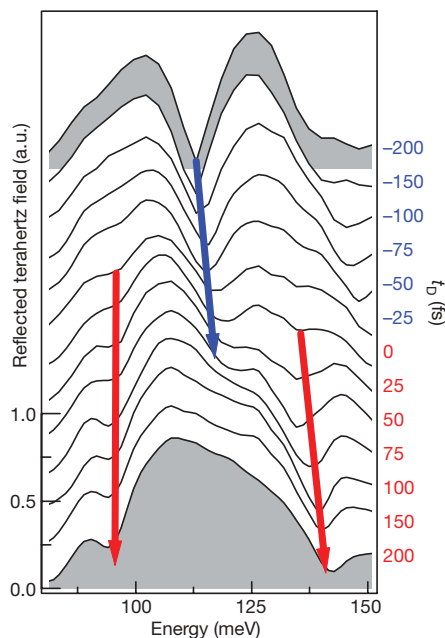
Figure 3 | Non-adiabatic switch-on dynamics of ultrastrongly coupled cavity polaritons. Spectra of the reflected terahertz field are given for various delay times, t_D (vertically off-set). The 12-fs control pulse ($\Phi = 0.1$ mJ cm^{-2}) arrives at $t_D = 0$. Blue arrow, bare cavity resonance; red arrows, ultrastrongly coupled intersubband cavity polariton branches.

qualitatively well described by the time dependence of the electron distribution in subband $|1\rangle$, as discussed in ref. 14.

Although light–matter coupling is turned on within femtoseconds, Ω_R remains constant on the subsequent nanosecond scale set by the recombination time of the electron–hole pairs. For practical device applications, our scheme may be extended to sub-cycle switch-off: a second infrared control pulse may, for example, promote photo-generated electrons from subband $|1\rangle$ into higher energy levels in

the conduction band, hence de-activating the intersubband transitions non-adiabatically. In an alternative, pump–dump, scheme, a pair of identical control pulses (each with pulse area π) may induce strong interband population inversion in subband $|1\rangle$ (switch-on of coupling) followed by ultrafast depopulation through stimulated interband emission (switch-off).

The extreme switching speed demonstrated in Fig. 3 entails unprecedented non-adiabatic phenomena, most strikingly seen in the time domain (Fig. 4). When a few-cycle probe transient (Fig. 4a) impinges on the unexcited modulator, part of its energy is directly reflected from the cavity surface. A second portion is evanescently coupled into the resonator, prepares a coherent photon state, and is subsequently re-emitted (Fig. 4b). This dynamics is encoded in the characteristic twin-pulse structure of the reflected transient (Fig. 4c). The initial burst is due to instantly reflected light whereas the second part results from re-emission. A time-frequency analysis corroborates this scenario. At each point, t, in time, we perform a numerical Fourier transform of the transient in Fig. 4c in a narrow window (width, 100 fs) centred about t. In this way, we map out the instantaneous spectral amplitude $E(t, \omega)$ as a function of time and photon energy (colour plot, Fig. 4c). Filling of the cavity manifests itself in a reflectance minimum at $\hbar\omega = 113$ meV ($t = 50$ fs), whereas subsequent cavity emission causes a delayed spectral peak at the same frequency.

The most intriguing situation arises when we turn light–matter coupling on while a coherent state of bare photons is still present inside the cavity (Fig. 4d): the control pulse (vertical arrow, Fig. 4d) abruptly alters Ω_R during the free cavity decay (second burst of reflected field). Notably, the emission of bare photons is interrupted on a timescale shorter than half an oscillation cycle of light, which is a compelling proof of non-adiabaticity. The subsequent field trace has a characteristic two-mode beating (shown magnified in Fig. 4e; see also Supplementary Fig. 1) and the corresponding spectra (colour plot, Fig. 4d) display minima at energies of 93 meV and 143 meV (indicated by the two diagonal arrows), which are hallmarks of the two polariton branches. Thus, we do not only control the eigenstates of the microcavity, but effectively convert a coherent photon population into ultrastrongly coupled cavity polaritons beating at the
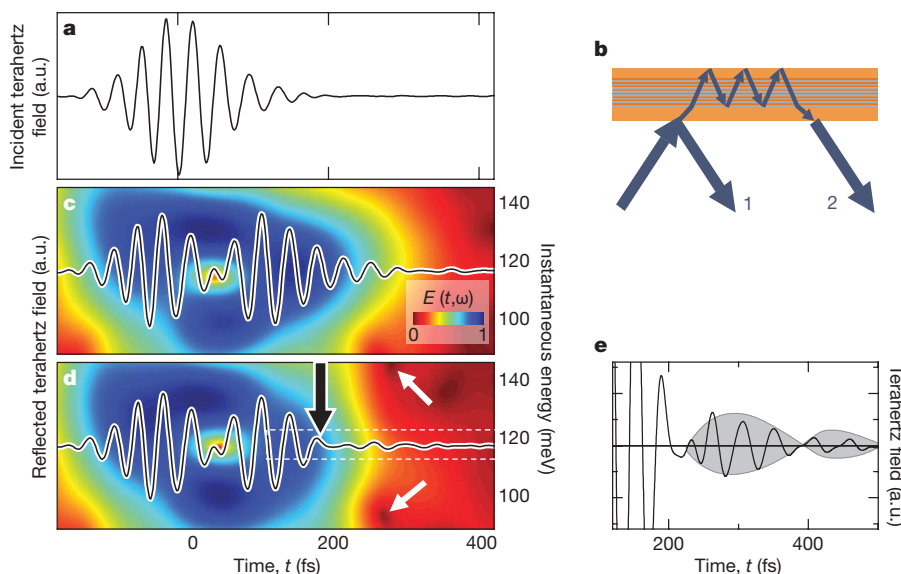
Figure 4 | Perturbed cavity decay. a, A measured few-cycle transient incident on the microcavity structure. **b**, Sketch of terahertz reflection from the cavity indicating two distinct contributions: (1) direct reflection at the first mirror of the cavity and (2) re-emission of coherent photon states inside the cavity give rise to a characteristic twin-pulse shape. **c**, Time trace of the experimentally determined terahertz field (black curve) reflected from the unexcited cavity. The corresponding instantaneous amplitude spectrum, $E(t, \omega)$ (colour-coded background: red, low field amplitude; blue, high field amplitude; see colour bar), is obtained as a function of photon energy and

time, t, by means of a wavelet transformation of the black curve. **d**, A 12-fs control pulse arrives within the coherence window of the cavity mode (black arrow). The reflected terahertz field (black curve) traces the non-adiabatic switch-on of ultrastrong light–matter coupling: The control pulse abruptly changes the exponential emission decay into a characteristic beating signature, on a sub-cycle scale. The corresponding spectrum (background colour plot) exhibits signatures of both polariton branches, at photon energies of 93 meV and 143 meV (white arrows). **e**, Beating signature (magnified view of dashed rectangle in **d**).

splitting frequency. We suggest the term 'perturbed cavity decay' to describe this non-adiabatic phenomenon.

Our experiments open a new domain of light–matter interaction at the ultrastrong and ultrafast limit. We have observed the dynamics of a coherent photon population during sub-cycle switching. The data provide a benchmark for the most recent, and future, theories of ultrastrong coupling and encourage a systematic search for non-adiabatic QED phenomena, such as the generation of quantum vacuum radiation, reminiscent of the dynamical Casimir effect or Hawking radiation of black holes[20,27,28]. A quantitative estimate using the theory of ref. 15 shows that for the switching times demonstrated (10^{-14} s), the number of vacuum photons released per pulse should be on the order of 10^3, a value that may be measurable with sensitive quantum detectors. Finally, our room-temperature, scalable and tunable semiconductor device, operated with low control fluence, may be highly relevant for next-generation ultrabroadband optical modulators. The concept may be combined with latest developments in robust, sub-10-fs telecommunications-compatible fibre lasers for real-world applications[29].

1. Raimond, J. M., Brune, M. & Haroche, S. Colloquium: Manipulating quantum entanglement with atoms and photons in a cavity. *Rev. Mod. Phys.* **73**, 565–582 (2001).
2. Brennecke, F. *et al.* Cavity QED with a Bose–Einstein condensate. *Nature* **450**, 268–271 (2007).
3. Weisbuch, C., Nishioka, M., Ishikawa, A. & Arakawa, Y. Observation of the coupled exciton-photon mode splitting in a semiconductor quantum microcavity. *Phys. Rev. Lett.* **69**, 3314–3317 (1992).
4. Dini, D., Köhler, R., Tredicucci, A., Biasiol, G. & Sorba, L. Microcavity polariton splitting of intersubband transitions. *Phys. Rev. Lett.* **90**, 116401 (2003).
5. Reithmaier, J. P. *et al.* Strong coupling in a single quantum dot-semiconductor microcavity system. *Nature* **432**, 197–200 (2004).
6. Chiorescu, I. *et al.* Coherent dynamics of a flux qubit coupled to a harmonic oscillator. *Nature* **431**, 159–162 (2004).
7. Anappara, A. A., Tredicucci, A., Beltram, F., Biasiol, G. & Sorba, L. Tunnel-assisted manipulation of intersubband polaritons in asymmetric coupled quantum wells. *Appl. Phys. Lett.* **89**, 171109 (2006).
8. Dupont, E., Gupta, J. A. & Liu, H. C. Giant vacuum-field Rabi splitting of intersubband transitions in multiple quantum wells. *Phys. Rev. B* **75**, 205325 (2007).
9. Hennessy, K. *et al.* Quantum nature of a strongly coupled single quantum dot-cavity system. *Nature* **445**, 896–899 (2007).
10. Schuster, D. I. *et al.* Resolving photon number states in a superconducting circuit. *Nature* **445**, 515–518 (2007).
11. Sapienza, L. *et al.* Electrically injected cavity polaritons. *Phys. Rev. Lett.* **100**, 136806 (2008).
12. Tsintzos, S. I., Pelekanos, N. T., Konstantinidis, G., Hatzopoulos, Z. & Savvidis, P. G. A. GaAs polariton light-emitting diode operating near room temperature. *Nature* **453**, 372–375 (2008).
13. Anappara, A. A. *et al.* Light-matter excitations in the ultra-strong coupling regime. Preprint at ⟨http://arxiv.org/abs/0808.3720⟩ (2008).
14. Ciuti, C., Bastard, G. & Carusotto, I. Quantum vacuum properties of the intersubband cavity polariton field. *Phys. Rev. B* **72**, 115303 (2005).
15. De Liberato, S., Ciuti, C. & Carusotto, I. Quantum vacuum radiation spectra from a semiconductor microcavity with a time-modulated vacuum Rabi frequency. *Phys. Rev. Lett.* **98**, 103602 (2007).
16. Purcell, E. M. Spontaneous emission probabilities at radio frequencies. *Phys. Rev.* **69**, 681 (1946).
17. Imamoglu, A., Ram, R. J., Pau, S. & Yamamoto, Y. Nonequilibrium condensates and lasers without inversion: Exciton-polariton lasers. *Phys. Rev. A* **53**, 4250–4253 (1996).
18. Kasprzak, J. *et al.* Bose–Einstein condensation of exciton polaritons. *Nature* **443**, 409–414 (2006).
19. Helm, M. in *Intersubband Transitions in Quantum Wells: Physics and Device Applications I* (eds Liu, H. C. & Capasso, F.) 1–99 (Academic, 2000).
20. Yablonovitch, E. Accelerating reference frame for electromagnetic waves in a rapidly growing plasma: Unruh-Davies-Fulling-DeWitt radiation and the nonadiabatic Casimir effect. *Phys. Rev. Lett.* **62**, 1742–1745 (1989).
21. Kübler, C., Huber, R., Tübel, S. & Leitenstorfer, A. Ultrabroadband detection of multi-THz field transients with GaSe electro-optic sensors: approaching the near infrared. *Appl. Phys. Lett.* **85**, 3360–3362 (2004).
22. Ferguson, B. & Zhang, X.-C. Materials for terahertz science and technology. *Nature Mater.* **1**, 26–33 (2002).
23. Tonouchi, M. Cutting-edge terahertz technology. *Nature Photon.* **1**, 97–105 (2007).
24. Huber, R. *et al.* How many-particle interactions develop after ultrafast excitation of an electron–hole plasma. *Nature* **414**, 286–289 (2001).
25. Kröll, J. *et al.* Phase-resolved measurements of stimulated emission in a laser. *Nature* **449**, 698–701 (2007).
26. Gaal, P. *et al.* Internal motions of a quasiparticle governing its ultrafast nonlinear response. *Nature* **450**, 1210–1213 (2007).
27. Unruh, W. G. Second quantisation in the Kerr metric. *Phys. Rev.* **10**, 3194–3205 (1974).
28. Hawking, S. W. Black hole explosions? *Nature* **248**, 30–31 (1974).
29. Sell, A. *et al.* Field-resolved detection of phase-locked infrared transients from a compact Er:fiber system tunable between 55 and 107 THz. *Appl. Phys. Lett.* **93**, 251107 (2008).

Author Information Reprints and permissions information is available at www.nature.com/reprints. Correspondence and requests for materials should be addressed to R.H. (rupert.huber@uni-konstanz.de).